
[View Journal Online](#)
[View Article Online](#)

Solvatochromism and ZINDO-IEFPCM solvation study on NHS ester activated AF514 and AF532 dyes: Evaluation of the dipole moments

Mallikarjun Kalagouda Patil ¹, Mare Goudar Kotresh ², Tarimakki Shankar Tilakraj ¹
 and Sanjeev Ramchandra Inamdar ^{1,*}

¹ Laser Spectroscopy Programme, Department of Physics, Karnatak University, Dharwad 580003, India

² Department of Physics, Vijayanagara Sri Krishnadevaraya University, Bellary 583104, India

* Corresponding author at: Laser Spectroscopy Programme, Department of Physics, Karnatak University, Dharwad 580003, India.
 e-mail: him_lax3@yahoo.com (S.R. Inamdar).

RESEARCH ARTICLE



doi 10.5155/eurjchem.13.1.8-19.2123

Received: 07 May 2021

Received in revised form: 23 October 2021

Accepted: 01 November 2021

Published online: 31 March 2022

Printed: 31 March 2022

KEYWORDS

DFT
 TD-DFT
 Dipole moment
 Alexa Fluor dyes
 Solvatochromism
 Natural bond orbital

ABSTRACT

In this study, the solvatochromic effect on the photophysical properties of Alexa Fluor 514 (AF514) and Alexa Fluor 532 (AF532) fluorescent dyes is examined experimentally and computationally. To explore the solvatochromism and dipole moments, the steady-state absorption and fluorescence spectra of the dyes were measured in a series of organic solvents. Various solvent correlation models, like Bilot-Kawski, Lippert-Mataga, Bakshiev, Kawski-Chamma-Viallet, and Reichardt microscopic solvent polarity parameters, were adapted to determine the dipole moments in their ground and excited states. For the computational investigation, the ground and excited-state geometries are optimized using density functional theory (DFT) and time-dependent density functional theory (TD-DFT), respectively, in vacuum. Furthermore, semiempirical ZINDO with the IEF-PCM model is used to evaluate the absorption transition energies of these dyes, which are comparatively studied in various solvent polarity along with experimental data. Additionally, the highest occupied molecular orbital energies (HOMO) and lowest unoccupied molecular orbital energies (LUMO), chemical softness, chemical hardness, energy gap, chemical potential, electronegativity, and molecular electrostatic potential (MEP) were estimated using DFT calculations at the CAM-B3LYP/6-311G(d,p) level, in gas phase. The experimental and computational results reveal that the singlet excited state dipole moment is greater than that of the ground state for the molecules considered. The angle between ground- and singlet excited-state dipole moments are found to be 0.50 and 0.49° making them almost parallel to each other. The natural bond orbital analysis (NBO) has been employed to investigate the stability of the molecule, inter- and intra-hyper-conjugative interactions and charge delocalization within the molecule.

Cite this: *Eur. J. Chem.* 2022, 13(1), 8-19

Journal website: www.eurjchem.com

1. Introduction

In the last few years, Alexa Fluor dyes and their bio-conjugates have generated remarkable interest in the field of surface energy transfer (SET), fluorescence resonance energy transfer (FRET), fluorescence bioimaging, and biosensing [1-4] due to their strong absorption spectra spanning the entire visible region, bright and photostable fluorescence, high quantum yields, long fluorescence lifetime, good water solubility and insensitivity of their absorption and fluorescence spectra over a broad range of pH values. Alexa Fluor 514 (AF514) and Alexa Fluor 532 (AF532) (Figure 1), respectively, are green and yellow fluorescent dyes that have been used successfully for analyzing/detecting analytes [5], detecting chromosomal aberrations [6,7], imaging cells [8,9], labeling amines/amino groups [10], labeling/detecting nucleic acids [11,12], probing the charge-transfer dynamics in DNA [11], and quantifying proteins *etc.* [13]

The spectral behavior of the solute molecule strongly depends on physical intermolecular solute-solvent interactions

(such as ion-dipole, dipole-induced dipole, and hydrogen bonding, *etc.*). The intermolecular force between the solute solvent depends on the physical properties of the solvent molecule, such as polarity, polarizability, dielectric constant, *etc.* There are important environmental factors that influence the position, intensities, and shape of the electronic spectra of the fluorophore. The ground and excited-state dipole moments of the fluorophore disclose information on its electronic and geometrical structure and the sharing of electrons in the relevant states. Therefore, studying the effect of solvents on the spectral behavior and dipole moments helps in extracting information about the excited state activities of the molecule. For the estimation of singlet excited-state dipole moment, various techniques are available such as electronic polarization of fluorescence [14], electronic dichroism [15], microwave conductivity [16], and stark splitting [17,18], but their use is restricted to comparatively simple molecules. Solvatochromism is one of the most widely used approaches to understand the effect of solvent and charge distributions in both ground and excited states [19-21].

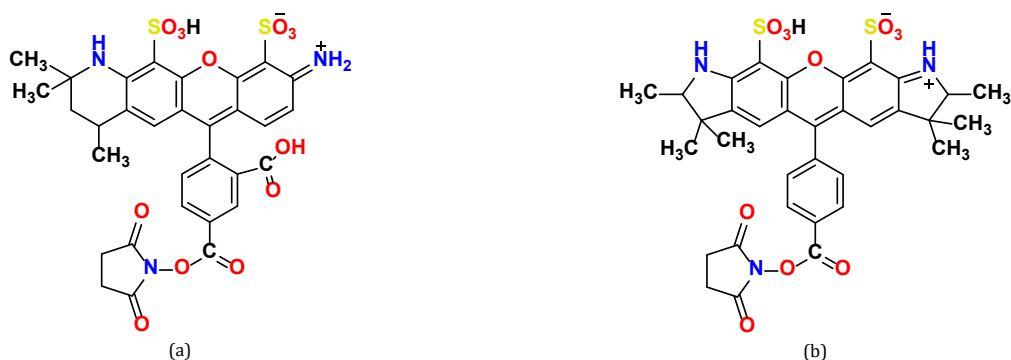


Figure 1. Molecular structures of Alexa Fluor 514 (a) and Alexa Fluor 532 dyes (b).

The dipole moment of fluorophore gives insight into the distribution of charge around the probe, the electron density, and the structure of the dye in solution. Hence, solvatochromism is an experimental endorsement of variations in the spectral behavior during electronic transitions and acts as important evidence for intramolecular charge transfer (ICT) in an excited state, and it plays an extensive role in research. In our previous studies, we have reported the computational and experimental investigations of solvent effect on Alexa Fluor 350 dye in a variety of solvent environments [22].

The effect of solvent polarity on the spectral behavior of the solute results in the shifting of the spectra depending on the fluorophore and the nature of the transition ($\sigma \rightarrow \sigma^*$, $n \rightarrow \sigma^*$, $\pi \rightarrow \pi^*$, and $n \rightarrow \pi^*$). The solvatochromic shift method is helpful to assign electronic transitions, in particular, $\pi \rightarrow \pi^*$ or $n \rightarrow \pi^*$. The transitions corresponding to $\pi \rightarrow \pi^*$ or $n \rightarrow \sigma^*$ are named positive and negative solvatochromism corresponding to bathochromic (red) and hypsochromic (blue) shift with increasing polarity of the solvents, respectively. The mixing of $\pi \rightarrow \pi^*$ or $n \rightarrow \pi^*$ transitions, leads to variations in the magnitude of dipole moments [23,24]. To explore various solvent properties, dielectric constant, refractive index, induced dipole moment, and relative permittivity, we have employed numerous methods through qualitative solvatochromism. Dimroth and Reichardt reported a simple approach to discriminate solvatochromism effectively in terms of an empirical solvent polarity parameter, $E_T(30)$, which is based on the negative solvatochromism of pyridinium N-phenolate-betaine dye [25]. To understand the solvatochromic shift through a single parameter, $E_T(30)$ values are calculated for all studied solvents [19].

To the best of our knowledge, investigations of the ground-state and excited-state dipole moments of AF514 and AF532 fluorescent dyes employing solvatochromism have not been reported in the literature. The previous reports deal with the use of these fluorophores in biological applications like identification of proteins, FRET, SET, and imaging cells, etc. Thus, it would be important and interesting to obtain information about the geometry and excited state activities of the molecule. In this framework, the present article aims to explore the influence of the solvent medium of varying polarity on the ground and excited state dipole moments. The investigation concerns the influence of alcohols and general solvents on electronic spectra of AF514 and AF532 dyes and the determination of ground and excited state dipole moments. Various solvent correlation techniques such as Bilot-Kawski [26], Lippert-Mataga [27,28], Bakshiev [29], Kawski-Chamma-Viallet [30,31] and microscopic solvent polarity parameter E_T^N were also used to examine the experimental results. Also, the value of ground-state dipole moments is computed by using density functional theory, while singlet excited state by time-dependent density functional theory formalism. Computational

solvatochromic analysis was carried out according to AM1/IEF-PCM and ZINDO/IEF-PCM for ground and excited states, respectively. Furthermore, natural bond orbital analysis was carried out to investigate the stabilization energy, hyper-conjugative interaction and charge delocalization within the studied molecules. The theoretically calculated dipole moments follow a similar trend with those estimated experimentally for both Alexa Fluor dyes.

2. Experimental

Alexa Fluor 514 and Alexa Fluor 532 were purchased from Thermo Fisher Scientific (Life Technologies, USA) and used without any further purification. All solvents used for the study are of the highest spectroscopic grade, purchased from Sigma-Aldrich (HPLC grade).

The absorption spectrum was measured using a UV-VIS-NIR spectrophotometer (JASCO, Model V-670) in the range of 300-700 nm. The PL spectra were recorded using a spectrofluorometer (JY Horiba, Model Fluoromax4). A quartz cuvette with a path length of 1 cm was used with both the excitation and emission slit widths fixed at 1 nm with integration time 0.1 s/nm. Data analysis was performed using OriginPro 8.0 software. Ground state optimization and excited state studies were carried out by adopting DFT and TD-DFT at the level of CAM-B3LYP/6-311G(d,p) basis set and solvent effects were simulated by implementing AM1-IEFPCM/ZINDO-IEFPCM using the Gaussian16 package.

3. Theoretical background

The ground and excited-state dipole moments of the solute provide information about the change in charge distribution and excited-state activities upon excitation. Several solvatochromic correlation methods have been used for AF514 and AF532.

3.1. Bilot-Kawski method

Bilot and Kawski [26] obtained a quantum mechanical relation using absorption ($\bar{\nu}_a$) and fluorescence ($\bar{\nu}_f$) band shifts measured in different solvents of varying permittivity (ϵ) and refractive index (n). Accordingly, the absorption ($\bar{\nu}_a$) and fluorescence ($\bar{\nu}_f$) maxima (in cm^{-1}) can be expressed by solvatochromism equations.

$$\bar{\nu}_a - \bar{\nu}_f = m_{B-K(1)} f(\epsilon, n) + \text{constant} \quad (1)$$

$$\bar{\nu}_a + \bar{\nu}_f = -m_{B-K(2)} [f(\epsilon, n) + 2g(n)] + \text{constant} \quad (2)$$

where $f(\varepsilon, n) = \frac{2n^2 + 1}{n^2 + 2} \left[\frac{\varepsilon - 1}{\varepsilon + 2} - \frac{n^2 - 1}{n^2 + 2} \right]$ and

$g(n) = \frac{3}{2} \left(\frac{n^4 - 1}{(n^2 + 2)^2} \right)$ are solvent polarity functions with the

permittivity of solvents (ε); refractive index (n), $m_{B-K(1)}$ and $m_{B-K(2)}$ are slopes obtained from the Equations (1) and (2), respectively, and are given below:

$$m_{B-K(1)} = \frac{2(\mu_e - \mu_g)^2}{hca^3} \quad (3)$$

$$\text{and } m_{B-K(2)} = \frac{2(\mu_e^2 - \mu_g^2)}{hca^3} \quad (4)$$

where c is the velocity of light in vacuum, 'a' the Onsager cavity radius of the solute, and h is the Planck's constant. Considering that symmetry of the solute molecule remains unchanged upon electronic transition, then ground state (μ_g) and excited state (μ_e) dipole moments are parallel [14]. In such cases μ_g and μ_e are given by

$$\mu_g = \frac{m_{B-K(2)} - m_{B-K(1)}}{2} \left(\frac{hca^3}{2m_{B-K(1)}} \right)^{\frac{1}{2}} \quad (5)$$

$$\mu_e = \frac{m_{B-K(2)} + m_{B-K(1)}}{2} \left(\frac{hca^3}{2m_{B-K(2)}} \right)^{\frac{1}{2}} \quad (6)$$

$$\text{and } \mu_e = \frac{m_{B-K(2)} + m_{B-K(1)}}{m_{B-K(2)} - m_{B-K(1)}} \mu_g \text{ for } m_{B-K(2)} > m_{B-K(1)} \quad (7)$$

Generally, the dipole moments (μ_g) and (μ_e) are not parallel to each other and make an angle ϕ between them, which can be estimated using Equation (8) [32]

$$\cos \phi = \frac{1}{2\mu_g\mu_e} \left[(\mu_e^2 + \mu_g^2) - \frac{m_{B-K(1)}}{m_{B-K(2)}} (\mu_e^2 - \mu_g^2) \right] \quad (8)$$

3.2. Lippert-Mataga, Bakshiev, and Kawski-Chamma-Viallet method

Experimental ground and singlet excited state dipole moments can also be determined by the solvatochromic methods given by Lippert-Mataga Equation (9) [27,28], Bakshiev Equation (10) [29] and Kawski-Chamma-Viallet Equation (11) [30,31],

$$\bar{\nu}_a - \bar{\nu}_f = m_{L-M} F_{L-M}(\varepsilon, n) + \text{Constant} \quad (9)$$

$$\bar{\nu}_a - \bar{\nu}_f = m_B F_B(\varepsilon, n) + \text{Constant} \quad (10)$$

$$\frac{\bar{\nu}_a + \bar{\nu}_f}{2} = -m_{K-C-V} F_{K-C-V}(\varepsilon, n) + \text{Constant} \quad (11)$$

where,

$$m_{L-M} = \frac{2(\mu_e - \mu_g)^2}{hca^3} \quad (12)$$

$$m_B = \frac{2(\mu_e - \mu_g)^2}{hca^3} \quad (13)$$

$$m_{K-C-V} = \frac{2(\mu_e^2 - \mu_g^2)}{hca^3} \quad (14)$$

m_{L-M} , m_B , m_{K-C-V} are slopes produced from plots $(\bar{\nu}_a - \bar{\nu}_f)$ vs F_{L-M} , F_B and $(\bar{\nu}_a + \bar{\nu}_f)/2$ vs F_{K-C-V} and F_{L-M} , F_B , F_{K-C-V} are solvent polarity functions given by Equations (15)-(17).

$$F_{L-M}(\varepsilon, n) = \frac{\varepsilon - 1}{2\varepsilon + 1} - \frac{n^2 - 1}{2n^2 + 1} \quad (15)$$

$$F_B(\varepsilon, n) = \frac{2n^2 + 1}{(n^2 + 2)} \left[\frac{\varepsilon - 1}{\varepsilon + 2} - \frac{n^2 - 1}{n^2 + 2} \right] \quad (16)$$

$$F_{K-C-V}(\varepsilon, n) = \left[\frac{2n^2 + 1}{2(n^2 + 2)} \left(\frac{\varepsilon - 1}{\varepsilon + 2} - \frac{n^2 - 1}{n^2 + 2} \right) + \frac{3(n^4 - 1)}{2(n^2 + 2)^2} \right] \quad (17)$$

3.3. Empirical microscopic solvent polarity parameter

The empirical microscopic solvent polarity parameter scale [E_T^N] proposed by Reichardt [19] correlates better with the spectral shift of molecule than the traditionally used technique based on bulk solvent polarity functions. The correlation between the microscopic solvent polarity parameter (E_T^N) with spectral shifts is given by

$$\bar{\nu}_a - \bar{\nu}_f = m E_T^N + \text{constant} \quad (18)$$

$$\text{with } m = 11307.6 \left[\left(\frac{\Delta\mu}{\Delta\mu_B} \right)^2 \left(\frac{a_B}{a} \right)^3 \right] \quad (19)$$

where $a_B = 6.2 \text{ \AA}$ and $\Delta\mu_B = 9 \text{ D}$ are radius of Onsager cavity and change in ground and excited state dipole moment of Betaine dye on excitation 'a' and $\Delta\mu$ correspond to Alexa Fluor molecules; E_T^N , the normalized solvent polarity function proposed by Reichardt [33] is a dimensionless solvatochromic parameter defined based on the absorption wave number $\bar{\nu}_a$ of a standard Betaine dye in the solvent.

$$E_T^N = \frac{E_T(\text{Solvent}) - E_T(\text{TMS})}{E_T(\text{Water}) - E_T(\text{TMS})} = \frac{E_T(\text{Solvent}) - 30.7}{32.4} \quad (20)$$

where TMS represents tetramethylsilane, E_T (solvent) empirical solvent polarity parameter ranges from 0 for TMS, to 1.000 for water extreme polar. Using these values, the change in dipole moments can be determined by Equation (21)

$$\Delta\mu = \mu_e - \mu_g = \left[\frac{m \times 81}{(6.2/a)^3 \times 11307.6} \right]^{1/2} \quad (21)$$

Table 1. Spectral and photophysical parameters of AF514 and AF532 in various solvent polarity.

Solvents	λ_{abs} (nm)				λ_{emi} (nm)		$\bar{\nu}_a$, cm ⁻¹		$\bar{\nu}_f$, cm ⁻¹		$\bar{\nu}_a - \bar{\nu}_f$, cm ⁻¹		$\bar{\nu}_a + \bar{\nu}_f$, cm ⁻¹		$(\bar{\nu}_a + \bar{\nu}_f)/2$, cm ⁻¹	
	AF514		AF532		AF514	AF532	AF514	AF532	AF514	AF532	AF514	AF532	AF514	AF532	AF514	AF532
	Exp.	Theor.*	Exp.	Theor.*												
Methanol	514	486	527	491	546	555	19455	18975	18315	18018	1140	957	37770	36993	18885	18496
Ethanol	517	488	528	493	553	552	19342	18939	18083	18115	1259	823	37425	37055	18712	18527
Butanol	518	492	531	492	541	561	19305	18832	18484	17825	820	1007	37789	36657	18894	18328
Hexanol	520	494	532	499	538	557	19230	18796	18587	17953	643	843	37818	36750	18909	18375
Decanol	521	499	532	503	539	558	19193	18796	18552	17921	640	875	37746	36718	18873	18359
Acetone	525	489	531	494	550	576	19047	18832	18181	17361	865	1471	37229	36193	18614	18096
Acetonitrile	519	487	526	503	542	558	19267	19011	18450	17921	817	1090	37718	36932	18859	18466
DMF	526	491	535	496	550	563	19011	18691	18181	17761	829	929	37193	36453	18596	18226
DMSO	529	490	539	495	551	568	18903	18552	18148	17605	754	947	37052	36158	18526	18079
Chloroform	528	504	531	508	550	549	18939	18832	18181	18214	757	617	37121	37047	18560	18523

*Theoretical values are estimated by Gaussian 16 With ZINDO/IEFPCM model.

where m is the slope of the linear plot of E_T^N vs. Stokes shift.

3.4. Onsager cavity radius

The value of the Onsager cavity radius 'a' of AF514 and AF532 was determined by using Equation (22) [34,35]

$$a = \left[\frac{3M}{4\pi\rho N_A} \right]^{1/3} \quad (22)$$

where N_A the Avogadro's number, ρ is the density and M molecular weight of the molecule. For studied molecules, $a_{(\text{AF514})} = 5.034 \text{ \AA}$ and $a_{(\text{AF532})} = 5.142 \text{ \AA}$, respectively.

3.5. Computational studies

The ground and excited state geometries of Alexa Fluor (AF514 and AF532) dyes were optimized using density functional theory and time-dependent density functional theory at the DFT/CAM-B3LYP/6-311G(d,p) and TD-DFT/CAM-B3LYP/6-311G(d,p) level in vacuum using Gaussian 16 software [36]. To explore the solvatochromism, the ground-state geometry of the fluorophores is optimized in all the solvents using semi-empirical method at the level AM1/IEF-PCM. ZINDO/IEF-PCM was used to obtain the transition energies and electronic absorption spectra in the solvent system. The ground and excited-state dipole moment vectors, HOMO, LUMO, and MEP maps are computed using DFT and TD-DFT, respectively.

4. Results and discussion

4.1. Solvent effect on the absorption and fluorescence spectra of AF514 and AF532 dyes

Steady-state absorption and fluorescence spectra of Alexa Fluor dyes were obtained in various solvents with different solvent polarities. Figure 2 shows the typical absorption and fluorescence spectra of AF514 and AF532 in alcohol and general solvents, respectively. The effects of solvent can bring major changes in the intensity, shape and position of the absorption and fluorescence bands, which signify whether excited or ground state is more stabilized with the solvent [37,38]. Hence, these changes are the result of a specific interaction between the solute-solvent molecules. The absorption and PL maxima in nanometers, wavenumber in cm⁻¹, and shift in spectra of AF514 and AF532 in different solvents are listed in Table 1. All the calculated parameters $f(\epsilon, n)$, $g(n)$, and $f(\epsilon, n) + 2g(n)$, and some physical constants, Reichardt parameter E_T^N are listed in Table 2.

Table 1 discloses the spectral position of the AF514 and AF532 dyes in various solvents. It is noticed that the absorption maxima of both dyes lie between (514-529) nm and (526-539) nm and exhibit a small magnitude of shift (15 nm for AF514 and 13 nm for AF532, respectively) between the selected solvents. In polar solvents (Methanol to decanol), the absorption maximum shifts from 514 to 521 nm and 527 to 532 nm for AF514 and AF532, respectively, leading to a red-shift or bathochromic shift. However, the fluorescence maxima of these dyes lie between (538-553) nm and (549-576) nm and show a slightly higher shift (15 and 27 nm for AF514 and AF532, respectively) in AF532 as compared to its excitation spectra. This suggests that both the AF514 and AF532 dyes are more stabilized in the singlet excited state (S1) relative to the ground state (S2). It means that the polarity of solvents has affected the ground-state energy of the molecule less as compared to the excited state. Consequently, the value for the ground-state dipole moment would be smaller compared to that of the excited state. The observed value of the Stokes shift varies from 1259 to 957 cm⁻¹ (for AF514) and 957 to 617 cm⁻¹ (for AF532) with the change in polarity of the solvents (Table 1). Varying Stokes shift with changing solvent polarity implies that solute solvent interactions are different in excited and ground states; indicating significant change in the ground state geometry of the dyes.

4.2. Estimation of dipole moments using solvatochromism of dyes

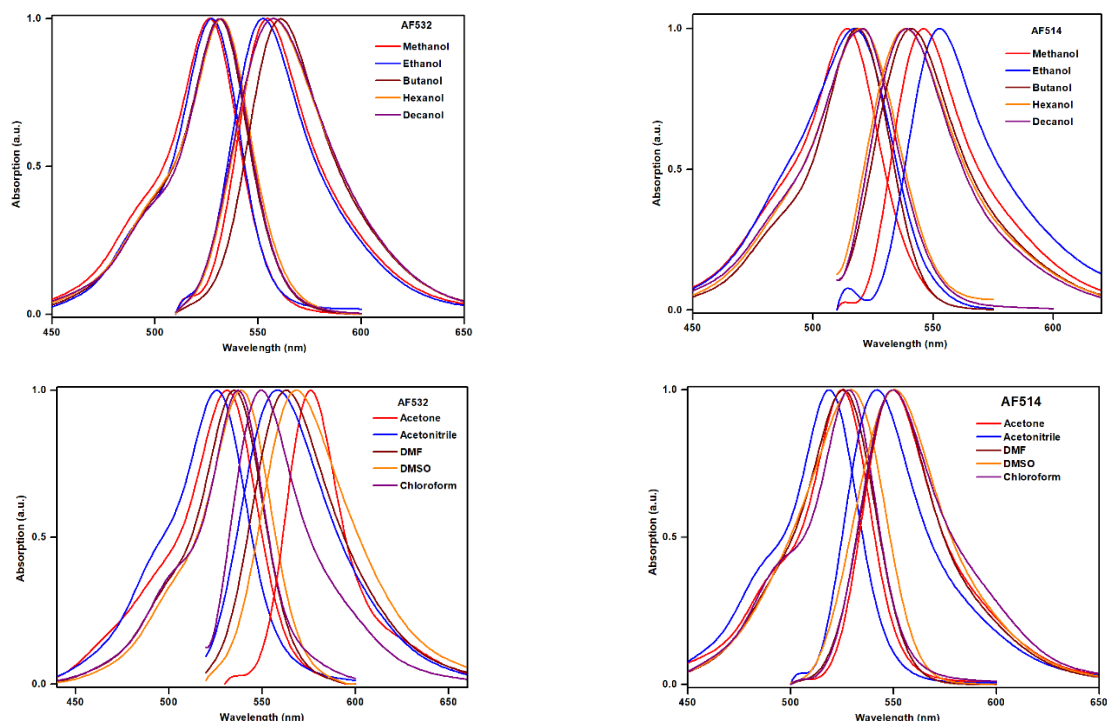
In solvatochromism, the dielectric constant (ϵ) and the refractive index (n) of solvents play a vital role in the spectral shift (Stokes shift). It means that the spectral shift is due to the specific interactions between solute-solvent molecules. It might be influenced by solvent parameters like hydrogen bond donor (HBD), hydrogen bond acceptor (HBA) and solvent polarity. To determine the dipole moments of these dyes various solvatochromism shift methods are used. The ground state dipole moment (μ_e) of AF514 and AF532 dyes were determined by Bilot-Kawski correlation (Equation (1)). The value of singlet excited state dipole moments of these dyes was determined by the correlation between shift in the spectra and solvent polarity as given by Bilot-Kawski (Equation (2)), Lippert-Mataga Equation (9), Bakhshiev Equation (10), Kawski-Chamma-Viallet Equation (11) and Reichardt correlation Equation (18). For both dyes, linear regression was carried out and the resulting data were fit into a straight line, whose slopes ($m_{B-K(1)}$, $m_{B-K(2)}$, m_{L-M} , m_B , m_{K-C-V} and m_R), intercepts and correlation coefficients are listed in Table 3. It is noticed that some solvents deviated from the linear fit, possibly due to short range solute-solvent interactions. It was observed that the correlation coefficients (R^2) of AF514 and AF532 are found to be in the range 0.811 to 0.979 and 0.798 to 0.991, respectively, which are achieved by using more solvents to obtain good linearity.

Table 2. Solvent parameters and calculated values for solvent polarity functions.

Solvent	n	ϵ	α	Π^*	β	E_T^N	$E_T(30)$	$f(\epsilon, n)$	$g(n)$	$f(\epsilon, n) + 2g(n)$	$f_{L-M}(\epsilon, n)$	$f_B(\epsilon, n)$	$f_{K-C-V}(\epsilon, n)$
Methanol	1.329	33.70	0.98	0.60	0.66	0.762	55.4	0.857	0.224	1.305	0.3090	0.8574	0.6528
Ethanol	1.369	24.30	0.86	0.54	0.75	0.654	51.9	0.812	0.245	1.303	0.2856	0.8092	0.6557
Butanol	1.399	17.40	0.84	0.84	0.47	0.586	49.7	0.749	0.271	1.291	0.2633	0.7494	0.6458
Hexanol	1.418	13.00	0.80	0.40	0.80	0.559	48.8	0.686	0.284	1.254	0.2431	0.6860	0.6269
Decanol	1.437	8.00	0.70	0.45	0.70	0.525	47.7	0.553	0.297	1.146	0.2041	0.5527	0.5727
DMSO	1.359	47.24	0.08	0.71	0.76	0.355	42.2	0.928	0.222	1.372	0.3038	0.8771	0.6830
DMF	1.430	38.25	0.00	0.88	0.69	0.386	43.2	0.792	0.245	1.281	0.2753	0.8394	0.7114
Acetonitrile	1.344	36.64	0.19	0.75	0.40	0.460	45.6	0.861	0.235	1.330	0.3049	0.8610	0.6648
Acetone	1.479	21.01	0.00	0.71	0.43	0.444	45.1	0.839	0.292	1.423	0.2442	0.7522	0.6999
Chloroform	1.446	4.89	0.44	0.00	0.58	0.259	39.1	0.370	0.302	0.975	0.1482	0.3708	0.4876

Table 3. Linear plot data of AF514 and AF532 obtained from different correlation methods.

Methods		Slope		Intercept		Correlation coefficient (R ²)		No. of data point	
		AF514	AF532	AF514	AF532	AF514	AF532	AF514	AF532
Bilot-Kawski	M _{B-K(1)}	145.39	803.25	705.29	321.69	0.862	0.826	04:10	07:10
Bilot-Kawski	M _{B-K(2)}	6385.27	2053.55	46101.35	39059.38	0.924	0.991	05:10	05:10
Lippert-Mataga	m _{L-M}	2772.75	2713.0	77.40	249.26	0.979	0.835	04:10	07:10
Bakhshiev	m _B	631.35	884.41	300.86	311.42	0.863	0.869	06:10	06:10
Kawski-Chamma-Viallet	m _{K-C-V}	5795.56	1218.50	22586.11	19104.12	0.842	0.887	06:10	05:10
Reichardt	m _R	753.89	617.83	537.13	482.62	0.811	0.798	06:10	05:10

**Figure 2.** Normalized absorption and emission spectra of AF514 and AF532 in alcohols and general solvents.

To determine the dipole moments experimentally, solvents correlation methods are used. The ground and excited state dipole moments (μ_g^c and μ_e^c) were calculated by using the slopes $m_{B-K(1)}$ and $m_{B-K(2)}$ of the Bilot-Kawski correlations using Equations (5) and (6). The values of the singlet excited state dipole moment were also determined from the slopes (m_{L-M} , m_B , m_{K-C-V} and m_R) of Lippert-Mataga, Bakshiev, Kawski-Chamma-Viallet and Reichardt correlations using Equations (15)-(17) and (21). The Onsager cavity radii of AF514 and AF532 are calculated using Edwards' atomic increment method [35], and are tabulated in Table 4.

Using Gaussian 16 software, the theoretical values of ground and singlet excited state dipole moments of AF514 and AF532 dyes were determined in vacuum. From Table 4, it is observed that the ground state dipole moments are found to be 16.15 D and 18.57 D while singlet excited state dipole moments are 16.61 D and 23.47 D, respectively. Also, it is noticed that for

both molecules singlet excited state dipole moments (μ_e) are higher relative to ground state dipole moments as obtained from DFT and TDDFT computations as well as from Bilot-Kawski correlation method. This might be due to the significant redistribution of charge density between the electronic states, intramolecular bonding with solvents, charge transfer, and the nature of geometrical changes between the electronic states. This designates that both AF514 and AF532 dyes are significantly more polar in their excited state relative to the ground state. Therefore, both the studied molecules are more reactive in an excited state when interacting with the solvent.

We have observed a comparatively good agreement between the excited state dipole moments determined by Bilot-Kawski, Lippert-Mataga, Bakshiev, Kawski-Chamma-Viallet and Reichardt correlation methods. From Table 4, it can be seen that for both AF514 and AF532 dyes the excited state dipole moments obtained from the Lippert-Mataga method are higher as compared with the values obtained by other methods, since

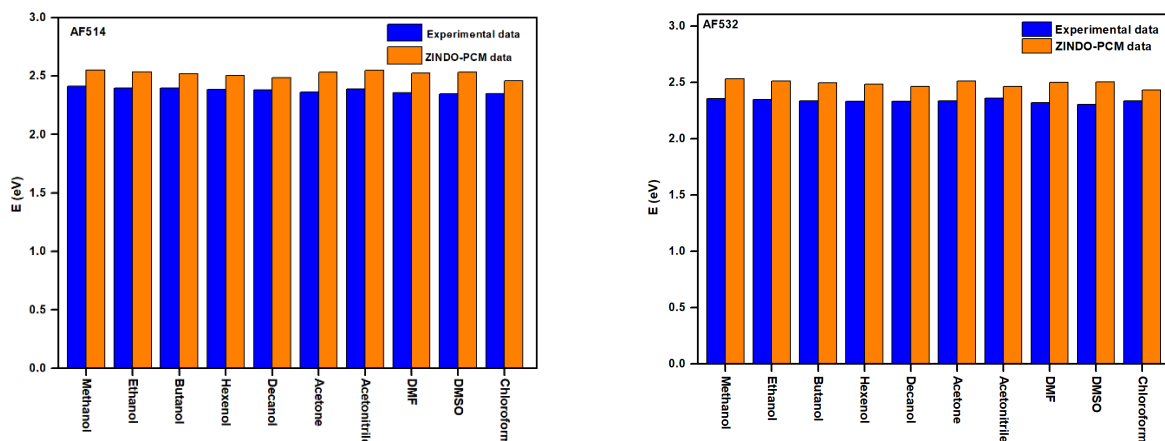


Figure 4. Comparison of experimental transition energies (eV) of AF514 and AF532 with computed by ZINDO-IEFPCM in different polarity of solvents.



Figure 5. Molecular electrostatic potential (MEP) maps of AF514 and AF532 in gas phase.

4.3.1. Solvatochromism via ZINDO/IEF-PCM method

The integral equation formalism polarizable continuum model (IEF-PCM) has been combined with the ZINDO semiempirical method to explain the effect of solvent on the geometry and electronic transitions of the molecule theoretically. The solvatochromic effect on electronic absorption maxima, transition energy, and oscillating strength of AF514 and AF532 has been computed and analyzed by ZINDO/IEF-PCM in all the solvents studied. The ZINDO/IEF-PCM method is one of the most popular tools for the calculation of excitation energies compared with other semiempirical methods, as seen in the earlier reports [40,41]. In this paper, the ZINDO/IEF-PCM calculations of these fluorescent dyes are gathered in Table 5. It is noticed that the experimentally obtained data (shift 18 and 17 nm) of the absorption maxima of both dyes replicate the same trend as compared with the ZINDO/IEF-PCM data (shift 15 and 13 nm) in all kinds of solvents. The dependence of molecules on solvent polarity and solute-solvent interaction energy are studied along with experimental data. Figure 4 gives the typical plot of E (eV) vs. solvents polarities for AF514 and AF532; resulting data are collected in Table 5. In addition, the table discloses the maximum and minimum difference in the electronic transition energy of AF514 and AF532 in all solvents studied both experimentally and computationally. From experimental interpretation, the maximum and minimum energy differences of AF514 and AF532 are found to be 0.137-0.103 eV and 0.176-0.131 eV in alcohols (methanol-decanol) and for general solvents (Acetone-Chloroform) and the computational study reveals them to be 0.186-0.110 eV and 0.203-0.094 eV, respectively. It can be noticed that the experimental and computed values are very close to each other. ZINDO/IEF-PCM examined electronic transition energies are well correlated with the experimental results with the minute differences of 0.137 eV for AF514 and 0.176 eV for AF532 dyes. Conversely, the experimentally obtained results for the same

are well-replicated for all the solvents. Oscillator strengths of AF514 and AF532 vary from 0.9205-0.8935 and 0.9160-0.8817 for alcohols and for other general solvents 0.9296-0.8947 and 0.9317-0.8467 as tabulated in Table 5.

4.3.2. Molecular electrostatic potential

The molecular electrostatic potential (MEP) is a widely used tool to explain the reactive behavior of a variety of chemical systems in various environments, helpful for the study of biological recognition processes and hydrogen bonding interactions [42]. The MEP of AF514 and AF532 were calculated using DFT at CAM-B3LYP/6-311G (d,p) basis set as shown in Figure 5. The red (negative) region of the MEP map was associated with electrophilic reactivity and blue (positive) is associated with nucleophilic reactivity. The MEP maps are found to be in the region of -0.08407 (red) and 0.08407 (blue) for AF514 and -0.08376 (red) and 0.08376 (blue) for AF532. Note that the electron density map of AF514 has a much larger range than that of AF532. The mapped MEP surface (Figure 5) confirms that the red region on the oxygen atoms of the sulfonic groups is an electron rich (more electronegative) region for both molecules studied. Oxygen atoms attached with pyrrolidinyl are less electronegative (yellow) relative to sulfonic group atoms. Therefore, oxygen is relatively electron rich and hydrogen is relatively electron deficient for AF514 and AF532 molecules, respectively.

4.3.3 Frontier molecular orbitals

The Frontier molecular orbital (FMO) analysis provides more useful information about the chemical reactivity and kinetic stability of the molecule. The frontier molecular orbitals called HOMO and LUMO of both studied molecules were investigated using DFT at the CAM-B3LYP/6-311G(d,p) basis set, in vacuum.

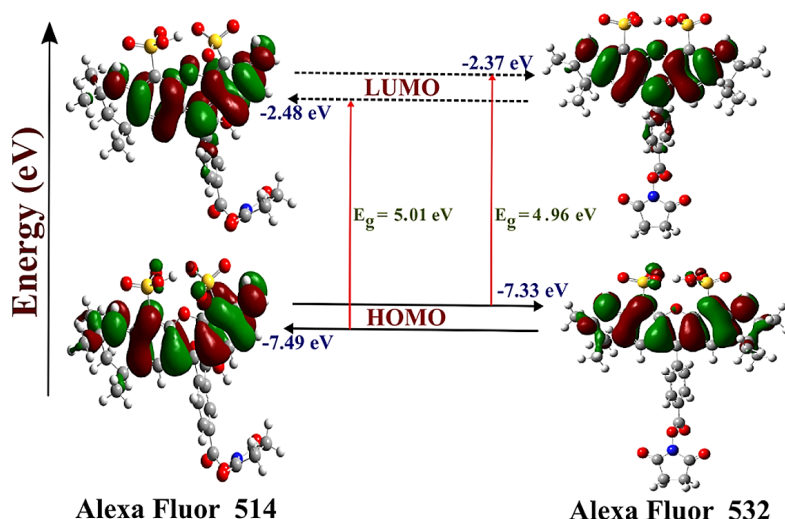


Figure 6. Frontier molecular orbitals of AF514 and AF532 in gas phase at CAM-B3LYP/6-311G (d,p) level.

As observed in AF514, in HOMO electrons are restricted to benzopyran, quinoline, amine and sulfonic groups attached with quinolin, whereas in LUMO electrons are localized on all the groups except dioxypyrrolidinyl, 2-methyl groups and sulfonic acid groups. As is seen from HOMO-LUMO, electrons are delocalized on the oxygen atom of the benzopyran group and a phenyl group. In AF532, in HOMO electrons are restricted to pyran, indol, and sulfonic groups, whereas in LUMO electrons are localized in pyran, indol, and phenyl groups. In addition, electrons are delocalized in the oxygen atom of the pyran group and phenyl group. For both the studied molecules electron density on the oxygen atom of benzopyran/pyran increases, at the same time electron density on oxygen atoms of sulfonic groups decreases during LUMO.

The energies of the HOMO and LUMO can be directly related to ionization potential and electron affinity, respectively [43]. The HOMO-LUMO energy values were computationally determined and revealed in Figure 6. For the dyes AF514 and AF532, HOMO-LUMO energy gap values were found to be 5.01 eV and 4.96 eV, respectively. The energy gap of AF532 is smaller than energy gap of AF514. This indicates that, the AF532 dye is highly reactive and has low kinetic stability as compared with AF514 dye. HOMO-LUMO energies are also used to find the softness (δ), chemical hardness (η), electron negativity (χ) and chemical potential (μ) of these molecules. For AF514 and AF532, the calculated values δ , η , χ , and μ are 0.399 eV⁻¹, 2.505 eV, -4.985 eV, 4.985 eV and 0.403 eV⁻¹, 2.480 eV, -4.850 eV, 4.850 eV, respectively. These values designate high excitation energy, high chemical activity, and good stability for the molecules studied.

4.3.4. Natural bond orbital (NBO) analysis

The NBO analysis is an effective tool to study intra- and inter-molecular bonding and interactions. It also provides important features of the molecular structure and a basis for the investigation of charge transfer or conjugative interactions in molecular systems. This in turn offers insight into the intramolecular, intermolecular bonding, and interaction among bonds [44,45]. Another useful chemical aspect of the natural bond orbital method is that it gives a favorable interaction of both filled/partially filled orbitals with nearby empty/virtual orbitals, which explains certain chemical phenomena in terms of donor-to-acceptor orbital interactions [46].

The NBO analysis is carried out to understand various second-order interactions between the 'filled' (donor) Lewis

type and 'vacant' (acceptor) non-Lewis type orbitals. NBO calculations were performed by using the NBO program as executed in the Gaussian 16 package at DFT/CAM-B3LYP/6-311G(d,p) basis set. The second-order Fock matrix was carried out to determine the donor-acceptor interactions in the NBO analysis [47]. Second order perturbation theory is used for the filled donor NBOs (i) and vacant acceptor NBOs (j), the stabilization energy $E(2)$ associated with $i(\text{donor}) \rightarrow j(\text{acceptor})$ delocalization can be obtained as given by,

$$E(2) = \Delta E_{ij} = q_i \frac{(F_{ij})^2}{(E_j - E_i)} \quad (23)$$

where F_{ij} is the off-diagonal NBO Fock matrix element between i and j , E_i and E_j are the energies of donor and acceptor orbitals of diagonal elements and q_i is the occupancy of the donor orbital, ΔE_{ij} is the difference in energy between the filled (donor) and the new lower energy orbital (formed by mixing of the donor and acceptor orbitals). In this NBO investigation, the higher $E(2)$ value, the interaction between electron donors and acceptors is more intensive and the extent of conjugation is greater.

The possible intensive perturbation energies of donor-acceptor interactions for AF514 and AF532 dyes are presented in Table 6. In AF532, the interactions between $\pi^*(\text{C}_6-\text{C}_7)$ and the antibonding acceptor $\pi^*(\text{C}_8-\text{C}_{10})$ have a strong interaction with the highest intramolecular charge transfer energy $E(2)$ value 284.13 kcal/mol. The lone pair electron donating $n \rightarrow \pi^*$ and $n \rightarrow \sigma^*$ transitions are observed between $n_1\text{N}_{19}$ to antibonding acceptor $\pi^*(\text{C}_4-\text{C}_5)$, $n_1\text{N}_{32}$ to $\pi^*(\text{O}_{30}-\text{C}_{33})$, $n_2\text{O}_{12}$ to $\pi^*(\text{C}_6-\text{C}_7)$ and $\pi^*(\text{C}_9-\text{C}_{12})$, $n_1\text{O}_{28}$ to $\sigma^*(\text{C}_{26}-\text{C}_{27})$, $n_2\text{O}_{29}$ to $\pi^*(\text{C}_{27}-\text{O}_{28})$, and $n_2\text{O}_{30}$ to $\sigma^*(\text{N}_{32}-\text{C}_{33})$ and $\sigma^*(\text{C}_{33}-\text{C}_{35})$ transitions are responsible for resonance in the molecule with intramolecular charge transfer interaction energy $E(2)$ value 86.27, 54.59, 40.95, 40.61, 20.44, 43.50, 37.86, and 24.64 kcal/mol, respectively. Although in AF514, the lone pair $n \rightarrow \pi^*$ transitions between $n_1\text{C}_5$ to $\pi^*(\text{C}_4-\text{C}_9)$ and $\pi^*(\text{C}_6-\text{C}_7)$, $n_1\text{C}_{11}$ to $\pi^*(\text{C}_8-\text{C}_{10})$, $\pi^*(\text{C}_{12}-\text{C}_{13})$ and $\pi^*(\text{C}_{15}-\text{C}_{16})$, $n_1\text{N}_{19}$ to $\pi^*(\text{O}_{36}-\text{O}_{38})$ and $\pi^*(\text{O}_{37}-\text{O}_{39})$ transitions are significant interactions responsible for the resonance in the molecule with stabilization energies of 41.14, 57.54, 103.82, 92.36, 62.53, 54.31, 51.92, and 43.91 kcal/mol, respectively. Hence, the stabilization energies of AF532 is larger than stabilization energy of AF514. This indicates the more intramolecular charge transfers in AF532 as compared with AF514. *i.e.*, AF532 is more stabilized relative to AF514.

Table 6. Analysis of Fock matrix using second order perturbation theory for the compounds AF514 and AF532 dyes.

Compound	Donor	Type	ED/e	Acceptor	Type	ED/e	E(2) ^a	E(j)-E(i) ^b	F(i,j) ^c
AF514	C4-C9	π	1.79133	C8-C10	π*	0.35249	16.92	0.38	0.074
	C6-C7	π	1.73596	C8-C10	π*	0.35249	12.47	0.39	0.063
	C8-C10	π	1.60720	C4-C9	π*	0.19437	25.19	0.40	0.095
	C8-C10	π	1.60720	C6-C7	π*	0.37639	41.19	0.36	0.109
	C27-C29	π	1.63579	C28-C30	π*	0.30184	25.83	0.37	0.089
	-	π	-	C31-C32	π*	0.35309	34.46	0.37	0.101
	-	π	-	C68-O70	π*	0.20239	14.50	0.41	0.072
	C31-C32	π	1.63990	C27-C29	π*	0.38236	28.81	0.37	0.092
	-	π	-	C28-C30	π*	0.30184	31.02	0.37	0.098
	-	π	-	C33-O35	π*	0.14640	13.00	0.45	0.073
	C5	n ₁ *	0.86568	C4-C9	π*	0.19437	41.14	0.21	0.113
	C5	n ₁ *	-	C6-C7	π*	0.37639	57.54	0.16	0.108
	C11	n ₁	1.10598	C8-C10	π*	0.35249	103.82	0.19	0.149
	C11	n ₁	-	C12-C13	π*	0.36417	92.36	0.19	0.138
	C11	n ₁	-	C15-C16	π*	0.20914	62.53	0.21	0.127
	C14	n ₁	0.86526	C12-C13	π*	0.36417	58.66	0.16	0.112
	C14	n ₁	-	C15-C16	π*	0.20914	45.61	0.19	0.112
	N19	n ₁	1.65778	O36-C38	π*	0.20780	54.31	0.41	0.138
	N19	n ₁	-	O37-C39	π*	0.20272	51.92	0.42	0.136
	O20	n ₂	1.72369	C6-C7	π*	0.37639	43.91	0.45	0.129
O20	n ₂	-	C12-C13	π*	0.36417	40.82	0.46	0.125	
AF532	C6-C7	π*	0.37639	C8-C10	π*	0.35249	284.13	0.01	0.088
	C3-C8	π	1.79416	C4-C5	π*	0.43630	25.65	0.37	0.093
	-	-	-	C6-C7	π*	0.47384	16.58	0.36	0.074
	C4-C5	π	1.63755	C6-C7	π*	0.47384	48.25	0.35	0.119
	-	-	-	C3-C8	π*	0.20085	13.31	0.40	0.068
	C6-C7	π	1.54132	C10-C11	π*	0.33650	40.33	0.36	0.112
	-	-	-	C3-C8	π*	0.20085	21.08	0.40	0.088
	-	-	-	C4-C5	π*	0.43630	15.21	0.35	0.066
	C9-C12	π	1.70818	C10-C11	π*	0.33650	13.44	0.38	0.064
	C10-C11	π	1.62847	C9-C12	π*	0.35870	36.73	0.37	0.105
	-	-	-	C14-C15	π*	0.18950	22.79	0.41	0.091
	-	-	-	C6-C7	π*	0.47384	15.63	0.35	0.068
	C14-C15	π	1.80240	C10-C11	π*	0.33650	17.22	0.38	0.075
	C21-C22	π	1.65230	C24-C26	π*	0.36271	33.80	0.37	0.100
	-	-	-	C23-C25	π*	0.28849	25.70	0.38	0.089
	C23-C25	π	1.63839	C21-C22	π*	0.34730	35.16	0.36	0.101
	-	-	-	C24-C26	π*	0.36271	29.34	0.36	0.092
	C24-C26	π	1.63839	C21-C22	π*	0.34730	28.15	0.36	0.091
	-	-	-	C23-C25	π*	0.28849	30.50	0.37	0.097
	-	-	-	C27-O28	π*	0.20068	23.94	0.37	0.087
	C13	n ₁ *	0.85834	C14-C15	π*	0.18958	44.47	0.20	0.116
	-	-	-	C9-C12	π*	0.35870	61.87	0.16	0.114
	O12	n ₂	1.71637	C6-C7	π*	0.47384	40.95	0.44	0.126
	-	-	-	C9-C12	π*	0.47384	40.61	0.47	0.125
N19	n ₁	1.65100	C4-C5	π*	0.43630	86.27	0.34	0.157	
O28	n ₂	1.83241	C26-C27	σ*	0.06309	20.44	0.82	0.119	
O29	n ₂	1.84634	C27-O28	π*	0.20068	43.50	0.48	0.130	
O30	n ₂	1.84677	N32-C33	σ*	0.10535	37.86	0.78	0.156	
O30	n ₂	-	C33-C35	σ*	0.06515	24.64	0.75	0.124	
N32	n ₁	1.66192	O30-C33	π*	0.20182	54.59	0.41	0.138	

^a E(2) is the stabilization energy in kJ/mol.^b Difference in energy (a.u.) between donor (i) and acceptor (j) NBO orbitals.^c F(i,j) is the Fock matrix element (a.u.) of the NBO orbitals.**Table 7.** NBO results showing the formation of Lewis and non-Lewis orbital for Alexa Fluor 514 dye.

Compound	Bond (A-B)	ED/energy (a.u.)	EDA%	EDB%	NBO	s %	p %
AF514	π C4-C9	1.79133	52.59	47.41	0.7252(sp ^{99.99})C+	0.01	99.92
	π C6-C7	1.73596	61.25	38.75	0.7826(sp ^{99.99})C+	0.08	99.89
	π C8-C10	1.60720	59.18	40.82	0.7693(sp ¹⁰⁰)C+	0.01	99.97
	π C12-C13	1.71092	40.70	59.30	0.6380(sp ¹⁰⁰)C+	0.00	99.93
	π C15-C16	1.80796	53.19	46.81	0.7293(sp ¹⁰⁰)C+	0.00	99.94
	π C27-C29	1.63579	47.70	52.30	0.6907(sp ¹⁰⁰)C+	0.01	99.96
	π C28-C30	1.62290	51.41	48.59	0.7170(sp ¹⁰⁰)C+	0.00	99.95
	π C31-C32	1.63990	46.13	53.87	0.6792(sp ¹⁰⁰)C+	0.00	99.95
	π C33-O35	1.98408	33.04	66.90	0.5748(sp ^{27.14})C+	3.54	96.00
	π O36-C38	1.99033	68.90	31.10	0.8300(sp ^{99.99})O+	0.04	99.83
	π O37-C39	1.98959	68.59	31.47	0.8278(sp ^{99.99})O+	0.22	99.65
	n ₁ *C5	0.86568	-	-	sp ¹⁰⁰	0.00	99.99
	n ₁ C5	1.10598	-	-	sp ¹⁰⁰	0.00	99.99
	n ₁ *C14	0.86526	-	-	sp ¹⁰⁰	0.00	100.00
	n ₁ N17	1.60446	-	-	sp ^{99.99}	0.17	99.81
	n ₁ N18	1.66606	-	-	sp ^{99.99}	0.04	99.94
	n ₁ N19	1.65776	-	-	sp ^{99.99}	0.68	99.93
	n ₂ O20	1.72369	-	-	sp ¹⁰⁰	0.01	99.93

Note: The symbols and labels appeared in the NBO analysis (Tables 6-8) were assigned according to the optimized structure as shown in Figure 4.

Table 8. NBO results showing the formation of Lewis and non-Lewis orbital for Alexa Fluor 532 dye.

Compound	Bond (A-B)	ED/energy (a.u.)	EDA%	EDB%	NBO	s %	p %
AF532	π C3-C8	1.79416	52.03	47.97	0.7213(sp ^{99.99})C+	0.02	99.93
	π C4-C5	1.63755	35.91	64.09	0.5993(sp ^{1.00})C+	0.00	99.93
	π C6-C7	1.54132	40.49	59.51	0.6363(sp ^{1.00})C+	0.00	99.96
	π C9-C12	1.70818	41.24	58.76	0.6422(sp ^{1.00})C+	0.00	99.93
	π C10-C11	1.62847	58.58	41.42	0.7654(sp ^{1.00})C+	0.00	99.97
	π C14-C15	1.80240	51.40	48.60	0.7170(sp ^{99.99})C+	0.03	99.91
	π C21-C22	1.65230	50.41	49.59	0.7100(sp ^{1.00})C+	0.00	99.96
	π C23-C25	1.63787	52.19	47.81	0.7224(sp ^{1.00})C+	0.00	99.95
	π C24-C26	1.63839	45.29	54.71	0.6730(sp ^{1.00})C+	0.00	99.95
	π C27-O28	1.98544	30.94	69.06	0.5562(sp ^{1.00})C+	0.00	99.46
	π O30-C33	1.99107	68.67	31.33	0.8286(sp ^{1.00})O+	0.00	99.86
	π O31-C34	1.99106	68.66	31.66	0.8286(sp ^{1.00})O+	0.00	99.86
	n_1^* C13	0.85834	-	-	Sp ^{99.99}	0.02	99.98
	n_2 O18	1.71637	-	-	Sp ^{99.99}	0.05	99.89
	n_1 N19	1.65100	-	-	Sp ^{63.07}	1.56	98.41
	n_1 N20	1.62467	-	-	Sp ^{35.95}	2.71	97.26
	n_2 O28	1.83241	-	-	sp ^{1.00}	0.00	99.91
	n_2 O29	1.84634	-	-	sp ^{1.00}	0.00	99.94
	n_2 O30	1.84677	-	-	sp ^{1.00}	0.00	99.92
	n_1 N32	1.66192	-	-	Sp ^{99.99}	0.37	99.62
	n_2 O45	1.79558	-	-	sp ^{1.00}	0.00	99.91
	n_2 O46	1.82894	-	-	Sp ^{99.99}	0.11	99.81
	n_2 O47	1.90071	-	-	Sp ^{99.99}	0.15	99.80
	n_2 O49	1.84079	-	-	sp ^{1.00}	0.01	99.92
	n_2 O50	1.80945	-	-	sp ^{1.00}	0.00	99.91

^a ED/e in a.u.

Tables 7 and 8 gives the occupancy of electrons and p-character in the significant NBOs of the studied molecules [44]. In AF514, the 100% p-character was observed in the lone pair n_1^* C₁₄. Except π bonding of (C₃₃-O₃₅) all the intense NBOs have the p-character very closer to 100%. Also, in AF532 except for lone pairs N₁₉ and N₂₀ all the significant NBOs have the p-character very closer to 100%.

5. Conclusion

Herein we report, the effect of solvents on steady-state absorption and fluorescence spectra of AF514 and AF532 dyes in various solvents of differing polarities. These data are used to understand the solvatochromic effect on spectral shift; estimate the ground and singlet excited state dipole moments by using various correlation methods and to compare with computational studies. The ground state dipole moment is estimated by Bilot-Kawski's method and singlet excited state dipole moments by employing Bilot-Kawski, Lippert-Mataga, Bakshiev, Kawski-Chamma-Viallet and Reichardt's methods. The dipole moments determined by using these correlation methods follow the same trend exhibited by theoretically calculated values using G16 software. Both experimental and computational results show that for these dyes singlet excited state dipole moment values are larger than those of ground state. This suggests that AF514 and AF532 are significantly more polar in the excited state than in their ground state. The ZINDO was adapted with integral equation formalism for the polarizable continuum model (IEF-PCM) to study the solvation potential and absorption transition energies. The experimental values of transition energy follow a similar trend exhibited by ZINDO/IEF-PCM model. The differences noticed in the transition energies are below 0.186 eV and 0.203 eV, respectively, in all the solvents. The small value of the HOMO-LUMO energy gap reveals the easy charge transfer interaction and softness of molecule. The intermolecular charge transfer between the bonding and antibonding orbitals and hybridization in the molecules under study has been understood by NBO analysis. It is observed that stabilization energies of AF532 are larger as compared with AF514 and it is more stable.

Acknowledgment

The authors would like to thank the University Grants Commission (UGC), New Delhi, India for the financial support under CPEPA (F.No.8-2/2008 (NS/PE)) and the USIC, Karnatak University, Dharwad for providing the UV-Vis Spectrophotometer. Gaussian calculations were performed in UPE-FAR-I Molecular Modelling Lab., Karnatak University, Dharwad. The author Mallikarjun would like to thank KSTePS Govt. of Karnataka for Providing DST-Ph.D. fellowship and Tarimakki Shankar Tilakraj is thankful to UGC for an SRF.

Disclosure statement

Conflict of interests: The authors declare that they have no conflict of interest. Ethical approval: All ethical guidelines have been adhered. Sample availability: Samples of the compounds are available from the author.

CRedit authorship contribution statement

Conceptualization: Sanjeev Ramchandra Inamdar, Mallikarjun Kalagouda Patil; Methodology: Mallikarjun Kalagouda Patil, Tarimakki Shankar Tilakraj, Mare Goudar Kotresh; Software: Mallikarjun Kalagouda Patil, Tarimakki Shankar Tilakraj; Validation: Mallikarjun Kalagouda Patil; Formal Analysis: Mallikarjun Kalagouda Patil, Tarimakki Shankar Tilakraj, Mare Goudar Kotresh; Investigation: Mallikarjun Kalagouda Patil, Tarimakki Shankar Tilakraj, Mare Goudar Kotresh, Sanjeev Ramchandra Inamdar; Resources: Mallikarjun Kalagouda Patil, Mare Goudar Kotresh; Data Curation: Mallikarjun Kalagouda Patil, Mare Goudar Kotresh; Writing - Original Draft: Mallikarjun Kalagouda Patil; Writing - Review and Editing: Mallikarjun Kalagouda Patil, Tarimakki Shankar Tilakraj, Mare Goudar Kotresh, Sanjeev Ramchandra Inamdar; Visualization: Mallikarjun Kalagouda Patil, Mare Goudar Kotresh, Sanjeev Ramchandra Inamdar; Funding acquisition: Sanjeev Ramchandra Inamdar; Supervision: Sanjeev Ramchandra Inamdar; Project Administration: Sanjeev Ramchandra Inamdar.

ORCID and Email

Mallikarjun Kalagouda Patil

 mkpatilphy@gmail.com

 <https://orcid.org/0000-0001-7126-9486>

Mare Goudar Kotresh

 kotreshm26@gmail.com

 <https://orcid.org/0000-0001-8738-2221>

Tarimakki Shankar Tilakraj

 tstilakraj1@gmail.com

 <https://orcid.org/0000-0001-5719-3593>

Sanjeev Ramchandra Inamdar

 him_lax3@yahoo.com <https://orcid.org/0000-0003-3398-4897>

References

- Patil, M. K.; Kotresh, M. G.; Inamdar, L. S.; Inamdar, S. R. Multidonor Surface Energy Transfer from Alexa Fluor Dyes to Gold Nanoparticles: A Quest for Innovative Sensor Applications. *J. Nanophotonics* **2020**, *14* (03), 036006.
- Conroy, E. M.; Li, J. J.; Kim, H.; Algar, W. R. Self-Quenching, Dimerization, and Homo-FRET in Hetero-FRET Assemblies with Quantum Dot Donors and Multiple Dye Acceptors. *J. Phys. Chem. C Nanomater. Interfaces* **2016**, *120* (31), 17817–17828.
- Grate, J. W.; Mo, K.-F.; Shin, Y.; Vasdekis, A.; Warner, M. G.; Kelly, R. T.; Orr, G.; Hu, D.; Dehoff, K. J.; Brockman, F. J.; Wilkins, M. J. Alexa Fluor-Labeled Fluorescent Cellulose Nanocrystals for Bioimaging Solid Cellulose in Spatially Structured Microenvironments. *Bioconjug. Chem.* **2015**, *26* (3), 593–601.
- Kim, H.; Ng, C. Y. W.; Algar, W. R. Quantum Dot-Based Multidonor Concentric FRET System and Its Application to Biosensing Using an Excitation Ratio. *Langmuir* **2014**, *30* (19), 5676–5685.
- Green, D. P. L.; Rawle, C. B. Analysis system and method, PCT Int. Appl. WO 2009082242, 2009.
- Hauke, S. Method for detecting a chromosomal aberration, PCT Int. Appl. WO 2012150022, 2012.
- Poulsen, T. S.; Poulsen, S. M.; Petersen, K. H. Methods for detecting chromosome aberrations, PCT Int. Appl. WO 2005111235, 2005.
- Tadross, M. R.; Park, S. A.; Veeramani, B.; Yue, D. T. Robust Approaches to Quantitative Ratiometric FRET Imaging of CFP/YFP Fluorophores under Confocal Microscopy. *J. Microsc.* **2009**, *233* (1), 192–204.
- Bestvater, F.; Spiess, E.; Stobrawa, G.; Hacker, M.; Feurer, T.; Porwol, T.; Berchner-Pfannschmidt, U.; Wotzlaw, C.; Acker, H. Two-Photon Fluorescence Absorption and Emission Spectra of Dyes Relevant for Cell Imaging. *J. Microsc.* **2002**, *208* (Pt 2), 108–115.
- Wayment, J. R.; Harris, J. M. Controlling Binding Site Densities on Glass Surfaces. *Anal. Chem.* **2006**, *78* (22), 7841–7849.
- Kawai, K.; Matsutani, E.; Maruyama, A.; Majima, T. Probing the Charge-Transfer Dynamics in DNA at the Single-Molecule Level. *J. Am. Chem. Soc.* **2011**, *133* (39), 15568–15577.
- Li, J.; Lee, J.-Y.; Yeung, E. S. Quantitative Screening of Single Copies of Human Papilloma Viral DNA without Amplification. *Anal. Chem.* **2006**, *78* (18), 6490–6496.
- Pihlasalo, S.; Engbert, A.; Martikkala, E.; Ylander, P.; Hänninen, P.; Härmä, H. Nonspecific Particle-Based Method with Two-Photon Excitation Detection for Sensitive Protein Quantification and Cell Counting. *Anal. Chem.* **2013**, *85* (5), 2689–2696.
- Kawski, A. Progress in photochemistry and photophysics, Ed. Rabek, J. F., CRC Press Boca Raton, Boston, Vol. V. pp. 1-47, 1992.
- Liptay, W. Dipole Moments and Polarizabilities of Molecules in Excited Electronic States. In *Excited States*; Lim, E. C., Ed.; Elsevier, 1974; Vol. 1, pp 129–229.
- Czekalla, J. Elektrische Fluoreszenzpolarisierung: Die Bestimmung von Dipolmomenten Angeregter Moleküle Aus Dem Polarisationsgrad Der Fluoreszenz in Starken Elektrischen Feldern. *Ber. Bunsenges. Phys. Chem.* **1960**, *64* (10), 1221–1228.
- Lombardi, J. R. Correlation between Structure and Dipole Moments in the Excited States of Substituted Benzenes. *J. Am. Chem. Soc.* **1970**, *92* (7), 1831–1833.
- Baumann, W.; Rossiter, B.W.; Hamilton, J.F. (Ed.) Physical Methods of Chemistry, vol. 38, John Wiley and Sons, New York, 1989.
- Reichardt, C. Solvatochromic Dyes as Solvent Polarity Indicators. *Chem. Rev.* **1994**, *94* (8), 2319–2358.
- Suppan, P. Invited Review Solvatochromic Shifts: The Influence of the Medium on the Energy of Electronic States. *J. Photochem. Photobiol. A Chem.* **1990**, *50* (3), 293–330.
- Mehata, M. S.; Singh, A. K.; Sinha, R. K. Experimental and Theoretical Study of Hydroxyquinolines: Hydroxyl Group Position Dependent Dipole Moment and Charge-Separation in the Photoexcited State Leading to Fluorescence. *Methods Appl. Fluoresc.* **2016**, *4* (4), 045004.
- Patil, M. K.; Kotresh, M. G.; Inamdar, S. R. A Combined Solvatochromic Shift and TDDFT Study Probing Solute-Solvent Interactions of Blue Fluorescent Alexa Fluor 350 Dye: Evaluation of Ground and Excited State Dipole Moments. *Spectrochim. Acta A Mol. Biomol. Spectrosc.* **2019**, *215*, 142–152.
- Mehata, M. S.; Singh, A. K.; Sinha, R. K. Investigation of Charge-Separation/Change in Dipole Moment of 7-Azaindole: Quantitative Measurement Using Solvatochromic Shifts and Computational Approaches. *J. Mol. Liq.* **2017**, *231*, 39–44.
- Young, J. W.; Pozun, Z. D.; Jordan, K. D.; Pratt, D. W. Excited Electronic State Mixing in 7-Azaindole. Quantitative Measurements Using the Stark Effect. *J. Phys. Chem. B* **2013**, *117* (49), 15695–15700.
- Reichardt, C. *Solvents and Solvent Effects in Organic Chemistry*, 3rd ed.; Wiley-VCH Verlag: Weinheim, Germany, 2006.
- Bilot, L.; Kawski, A. Zur Theorie Des Einflusses von Lösungsmitteln Auf Die Elektronspektren Der Moleküle. *Z. Naturforsch. A* **1962**, *17* (7), 621–627.
- Lippert, E. Dipolmoment Und Elektronenstruktur von Angeregten Molekülen. *Z. Naturforsch. A* **1955**, *10* (7), 541–545.
- Mataga, N.; Kaifu, Y.; Koizumi, M. Solvent Effects upon Fluorescence Spectra and the Dipolemoments of Excited Molecules. *Bull. Chem. Soc. Jpn.* **1956**, *29* (4), 465–470.
- Bakhshiev, N. G. Universal intermolecular interactions and their effect on the position of the electronic spectra of molecules in two component solutions, *Opt. Spektrosk.* **1964**, *16*, 821–832.
- Chamma, A.; Viallet, P. Determination du moment dipolaire d'une moleculédans un etat excite singulet. *Comptes Rendus de l'Academie des Sciences Paris Series C* **1970**, *270*, 1901–1904.
- Kawaski, A. Zur lösungsmittelabhängigkeit der Wellenzahl von Elektronenbanden lumineszierender Moleküle and über die Bestimmung der elektrischen Dipolomente im Anregungszustand, *Acta Phys. Polon.* **1966**, *29*, 507–518.
- Kawski, A. On the Estimation of Excited-State Dipole Moments from Solvatochromic Shifts of Absorption and Fluorescence Spectra. *Z. Naturforsch. A* **2002**, *57* (5), 255–262.
- Ravi, M.; Soujanya, T.; Samanta, A.; Radhakrishnan, T. P. Excited-State Dipole Moments of Some Coumarin Dyes from a Solvatochromic Method Using the Solvent Polarity Parameter, *E N T. J. Chem. Soc. Faraday Trans* **1995**, *91* (17), 2739–2742.
- Suppan, P. Excited-State Dipole Moments from Absorption/Fluorescence Solvatochromic Ratios. *Chem. Phys. Lett.* **1983**, *94* (3), 272–275.
- Edward, J. T. Molecular Volumes and the Stokes-Einstein Equation. *J. Chem. Educ.* **1970**, *47* (4), 261–270.
- Frisch, M. J.; Trucks, G. W.; Schlegel, H. B.; Scuseria, G. E.; Robb, M. A.; Cheeseman, J. R.; Montgomery, Jr., J. A.; Vreven, T.; Kudin, K. N.; Burant, J. C.; Millam, J. M.; Iyengar, S. S.; Tomasi, J.; Barone, V.; Mennucci, B.; Cossi, M.; Scalmani, G.; Rega, N.; Petersson, G. A.; Nakatsuji, H.; Hada, M.; Ehara, M.; Toyota, K.; Fukuda, R.; Hasegawa, J.; Ishida, M.; Nakajima, T.; Honda, Y.; Kitao, O.; Nakai, H.; Klene, M.; Li, X.; Knox, J. E.; Hratchian, H. P.; Cross, J. B.; Bakken, V.; Adamo, C.; Jaramillo, J.; Gomperts, R.; Stratmann, R. E.; Yazyev, O.; Austin, A. J.; Cammi, R.; Pomelli, C.; Ochterski, J. W.; Ayala, P. Y.; Morokuma, K.; Voth, G. A.; Salvador, P.; Dannenberg, J. J.; Zakrzewski, V. G.; Dapprich, S.; Daniels, A. D.; Strain, M. C.; Farkas, O.; Malick, D. K.; Rabuck, A. D.; Raghavachari, K.; Foresman, J. B.; Ortiz, J. V.; Cui, Q.; Baboul, A. G.; Clifford, S.; Cioslowski, J.; Stefanov, B. B.; Liu, G.; Liashenko, A.; Piskorz, P.; Komaromi, I.; Martin, R. L.; Fox, D. J.; Keith, T.; Al-Laham, M. A.; Peng, C. Y.; Nanayakkara, A.; Challacombe, M.; Gill, P. M. W.; Johnson, B.; Chen, W.; Wong, M. W.; Gonzalez, C.; and Pople, J. A.; Gaussian 16, Gaussian, Inc., Wallingford CT, 2016.
- Najare, M. S.; Patil, M. K.; Mantur, S.; Nadaf, A. A.; Inamdar, S. R.; Khazi, I. A. M. Highly Conjugated D-π-A-π-D Form of Novel Benzo[b] Thiophene Substituted 1,3,4-oxadiazole Derivatives; Thermal, Optical Properties, Solvatochromism and DFT Studies. *J. Mol. Liq.* **2018**, *272*, 507–519.
- Mishra, A. K.; Dogra, S. K. Effect of Solvents and PH on the Absorption and Fluorescence Spectra of 2-Phenylbenzimidazole. *Spectrochim. Acta A* **1983**, *39* (7), 609–611.
- Gülseven Sidir, Y.; Sidir, İ. Solvent Effect on the Absorption and Fluorescence Spectra of 7-Acetoxy-6-(2,3-Dibromopropyl)-4,8-Dimethylcoumarin: Determination of Ground and Excited State Dipole Moments. *Spectrochim. Acta A Mol. Biomol. Spectrosc.* **2013**, *102*, 286–296.
- Caricato, M.; Mennucci, B.; Tomasi, J. Solvent Polarity Scales Revisited: A ZINDO-PCM Study of the Solvatochromism of Betaine-30. *Mol. Phys.* **2006**, *104* (5–7), 875–887.
- Caricato, M.; Mennucci, B.; Tomasi, J. Solvent Effects on the Electronic Spectra: An Extension of the Polarizable Continuum Model to the ZINDO Method. *J. Phys. Chem. A* **2004**, *108* (29), 6248–6256.
- Okulik, N.; Jubert, A. H. Theoretical Analysis of the Reactive Sites of Non-steroidal Anti-inflammatory Drugs, *Internet Electron. J. Mol. Des.* **2005**, *4* (1), 17–30.
- Fukui, K. Role of Frontier Orbitals in Chemical Reactions. *Science* **1982**, *218* (4574), 747–754.
- Snehalatha, M.; Ravikumar, C.; Hubert Joe, I.; Sekar, N.; Jayakumar, V. S. Spectroscopic Analysis and DFT Calculations of a Food Additive Carmoisine. *Spectrochim. Acta A Mol. Biomol. Spectrosc.* **2009**, *72* (3), 654–662.
- Weinhold, F.; Landis, C. R. Natural Bond Orbitals and Extensions of Localized Bonding Concepts. *Chem. Educ. Res. Pr.* **2001**, *2* (2), 91–104.
- Wazzan, N. A.; Al-Qurashi, O. S.; Faidallah, H. M. DFT/ and TD-DFT/PCM Calculations of Molecular Structure, Spectroscopic Characterization, NLO and NBO Analyses of 4-(4-Chlorophenyl) and 4-[4-(Dimethylamino) Phenyl]-2-Oxo-1,2,5,6-Tetrahydrobenzo[h] Quinoline-3-Carbonitrile Dyes. *J. Mol. Liq.* **2016**, *223*, 29–47.

- [47]. Reed, A. E.; Curtiss, L. A.; Weinhold, F. Intermolecular Interactions from a Natural Bond Orbital, Donor-Acceptor Viewpoint. *Chem. Rev.* **1988**, *88* (6), 899–926.



Copyright © 2022 by Authors. This work is published and licensed by Atlanta Publishing House LLC, Atlanta, GA, USA. The full terms of this license are available at <http://www.eurjchem.com/index.php/eurjchem/pages/view/terms> and incorporate the Creative Commons Attribution-Non Commercial (CC BY NC) (International, v4.0) License (<http://creativecommons.org/licenses/by-nc/4.0>). By accessing the work, you hereby accept the Terms. This is an open access article distributed under the terms and conditions of the CC BY NC License, which permits unrestricted non-commercial use, distribution, and reproduction in any medium, provided the original work is properly cited without any further permission from Atlanta Publishing House LLC (European Journal of Chemistry). No use, distribution or reproduction is permitted which does not comply with these terms. Permissions for commercial use of this work beyond the scope of the License (<http://www.eurjchem.com/index.php/eurjchem/pages/view/terms>) are administered by Atlanta Publishing House LLC (European Journal of Chemistry).